Performance Study of a Ducted Fan System

Anita I. Abrego, Aerospace Engineer
aabrego@mail.arc.nasa.gov
NASA Ames Research Center
Moffett Field, CA

Robert W. Bulaga, Chief Engineer
rbulaga@millenniumjet.com
Millennium Jet Incorporated
Sunnyvale, CA

Abstract

An experimental investigation was completed in the NASA Ames 7- by 10-Foot Wind Tunnel with the objective of determining the performance characteristics of a ducted fan. The model was an annular duct with a 38-in diameter, 10-in chord, and a 5-bladed fixed-pitch fan. Model variations included duct angle of attack, exit vane flap length, flap deflection angle, and duct chord length. Duct performance data were obtained for axial and forward flight test conditions. Axial flow test data showed figure of merit decreases with increasing advance ratio. Forward flight data showed an increasing propulsive force with decreasing duct angle of attack. Exit vane flap deflection angle and flap chord length were shown to be an effective way of providing side force. Extending the duct chord did not effect the duct performance.

Notation

A_e	Duct exit area, ft^2
c_d	Duct chord, ft
C_L	Lift coefficient, L/qd_ec_d
C_P	Power coefficient, $550P/\rho n^3 d^5$
C_T	Thrust coefficient, shaft axis, $T/\rho n^2 d^4$
C_X	Propulsive force coefficient, wind axis, $F_P/\rho n^2 d^4$
d	Fan diameter, ft
F_P	Propulsive force, wind axis, lb
FM	Figure of merit, $50(d/A_e^{1/2})(C_T^{3/2}/C_P)$, percent
J	Advance ratio, V_∞/nd
L	Lift, lb
n	Fan rotational speed, rps
N	Fan rotational speed, rpm
P	Fan shaft power, $2\pi(Q/12)N/33000$, hp
q	Freestream dynamic pressure, $1/2\rho V_\infty^2$, lb/ft^2
T	Thrust, lb
V_∞	Free-stream velocity, fps
α	Duct angle of attack, deg
δ	Vane flap deflection angle, deg
ρ	Mass density of air, $slugs/ft^3$

Introduction

Ducted fans, or shrouded propellers, hold promise as a devices for high static thrust propulsion systems. When compared to an isolated propeller of the same diameter and power loading, ducted propellers typically produce greater static thrust. In addition, the ducted fan system offers a supplementary safety feature attributed to enclosing the rotating fan in the duct, therefore making it an attractive option for various advanced unmanned air vehicle configurations or for small/personal air vehicles (Ref. 1).

In static conditions, the lift due to the fan acts vertically. Air is drawn into the duct and divides at a stagnation point. The duct cross-section acts like an airfoil where the resultant lift vectors of the duct are strongly canted towards the center of the duct. The vertical components of the vectors provide additional duct lift. In translational flight, the freestream airflow adds more complexity to the flow field. On both the upstream and downstream edges of the duct, the stagnation point moves towards the oncoming flow. The upstream side of the duct operates at a higher angle of attack, increasing the magnitude of the upstream lift vector. As well, the downstream side of the duct operates at a lower angle of attack, decreasing the magnitude of the lift vector. The combined vectors result in a net increase in duct translational lift. However, they also result in a pitching moment on the duct's leading edge and a horizontal force in the freestream airflow direction, referred to as duct translational drag.

Early ducted fan research indicated the benefits gained by ducting or shrouding a propeller in static conditions as reported in 1931 by Stipa (Ref. 2). Reference 3 reports guide nozzle research for hydraulic and aeronautical propellers. In the 1960's, hover and forward flight performance characteristics for a wing tip mounted, 4-foot diameter ducted fan were reported in Refs. 4 and 5. On the same model, duct exit vanes and horizontal stabilizers were studied as methods to alleviate longitudinal trim and control problems (Ref. 6) and the performance effects of changing fan blade angle for 0-deg duct angle were reported (Ref. 7). The aerodynamic characteristics of a 7-foot diameter ducted propeller were reported for variations of power, free-stream velocity, blade angle, and duct angle of attack (Ref. 8). A comprehensive performance study (Ref. 9) analyzed a large number of model variations, indicating the shroud exit area ratio as the more dominant design variable.

NASA Ames Research Center and Millennium Jet Inc. have collaborated on an experimental investigation to study the performance characteristics of a ducted fan, representative of that on the SoloTrek XFV (Ref. 1). The goal of this effort was to determine the duct performance for variations of fan and duct geometry, for axial and forward flight test conditions. This paper will present a review of the wind tunnel test and the duct performance results

Test Description

Installation
Figure 1 shows the test installation of the ducted fan in the 7- by 10-Foot Wind Tunnel at NASA Ames Research Center. The model was rigidly fixed to a support cradle and mounted to the wind tunnel turntable. The fan was attached to the drivetrain through a splined connection in the fan hub. The main support arm and two streamlined support arms provided duct support. The pre-existing model drive train and the desire to locate the duct near the center of the test section resulted in the model support cradle and motor being exposed above the tunnel floor. The fan was driven by a 125 HP, water-cooled, electric motor through two right-angle gearboxes. The wind tunnel turntable provided the duct angle of attack changes. Figure 2 illustrates the hover/axial flight and forward flight test orientations.

Fig. 1. Ducted fan test in the NASA Ames 7- by 10- Foot Wind Tunnel.
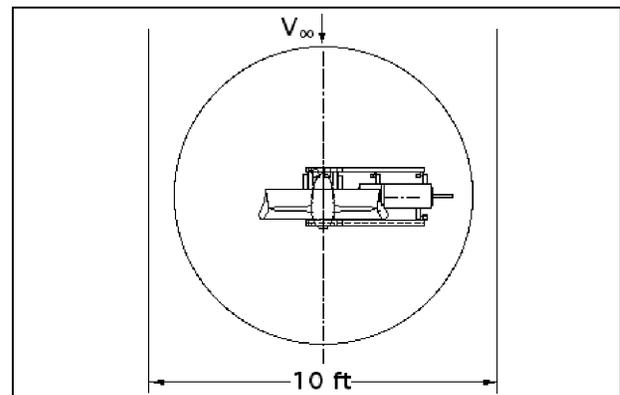
a) **Hover/axial flight orientation, α = +90 deg**
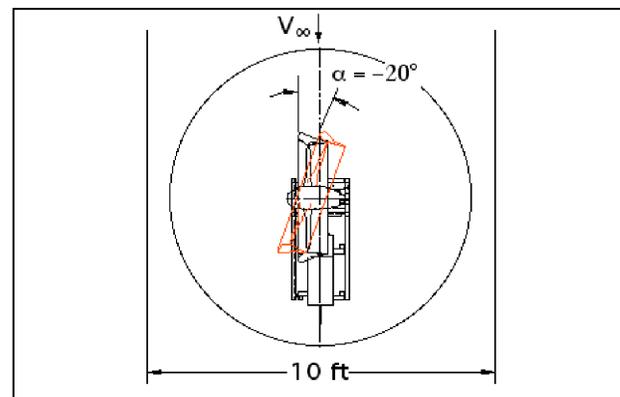
b) **Forward flight orientation, α = 0 deg (α = -20 deg indicates orientation of duct, not support structure)**

Fig. 2. Ducted fan model orientation.

Model

The model consisted of an annular duct with a five-bladed, fixed pitch fan. The duct had a 38-in inner diameter and a 10-in chord. Two 3-in chord vanes with 1-in flaps were located at the duct exit (Fig. 3). Exit vane flap deflection angle was manually adjustable to ±40 deg, in 10-deg increments. Baseline model parameters and variations in model geometry are shown in Table 1. Due to manufacturing defects, the fan tip clearance was not constant along the duct circumference. Tip clearance variations included 0.123 in at the top and 0.207 in at the bottom of the duct. The smallest tip clearances were 0.065 and 0.060 in at the 4 and 7 o'clock positions, respectively. Reference 10 shows that, as tip-clearance ratios increase, the duct thrust drops off rapidly. However, it is not known to what degree the tip clearance variations effect the test results.

Fig. 3. Exit vane with 1-in flap

Instrumentation and Data Acquisition

Forces and moments on the model were measured using the wind-tunnel balance system. Motor (fan) rotational speed was measured using an optical trigger. Torque was measured with an instrumented moment arm that was attached to the motor casing. Main and streamlined support arm loads were instrumented with strain gages. Test section velocity was measured using two methods, the tunnel pressure rings and a vane anemometer. The vane anemometer was used for tunnel speeds below 40 ft/sec and the tunnel differential pressures were used for tunnel speeds above 40 ft/sec. In addition to the physical measurements of the model, tufts were applied to the duct, fan hub centerbody, and one fan blade to monitor the flow field of each respective element. Model wake and tunnel wall interactions were monitored with tufts applied to the tunnel walls. The data acquisition system simultaneously recorded each parameter for a period of 2 sec, at a sample rate of 1024 samples per sec per channel. Model forces

were averaged and used to calculate lift, thrust, and side force coefficients. The power input to the ducted fan was determined using the motor torque and rotation speed.

Table 1. Model parameters

	Parameter	Baseline	Variation
Duct	Inner diameter	38 in	
	Chord	10 in	15 in
	Duct length (chord/diameter)	25.4%	50.7%
	Expansion angle	6 deg	
Fan	No. of blades	5	
	Diameter	37.8 in	
	Hub-tip diameter ratio	0.211	
	Blade angle control	Fixed pitch	
	Blade angle at tip	14.5 deg	
	Tip clearance (clearance/diameter)	0.07% to 2.4%	
Exit Vane	Chord	3 in	
	Flap chord	1 in	2.25 in
	Flap angle	0 deg	±40 deg in 10 deg increments

Test Parameters

Duct performance data were acquired over a range of axial and cross-flow test conditions, as shown in Table 2. Primarily, the tests were directed toward varying fan rotation speed at a given duct angle and tunnel speed.

Table 2. Range of Test Conditions

Parameter	Axial	Forward Flight
V_∞ (ft/sec)	0 to 42	5 to 135
J	-0.11 to 0.25	0 to 1.14
N (rpm)	1800, 2000, 2200, 2400, 2600, 3000, 3400	1800, 2200, 2600, 3000
α (deg)	+90, -90	5, 0, -2, -5, -10, -15, -20, -25
δ (deg)	-40 to +40 10-deg increments	-40 to +40 10-deg increments

Axial testing represented both hover and vertical descent flight test conditions. Fan rotational speed was varied from 1800 to 3400 rpm, corresponding to a maximum tip speed of 564 ft/sec. Low advance ratios represented near-hover conditions, however, the model did generate significant flow through the tunnel. Therefore, the model was tested at ±90 deg angle of attack to create different axial flow conditions. At 90-deg angle of attack, the tunnel was run at low speeds to generate flow against the

model to achieve near-zero and even negative inflow.

Forward flight conditions relate to operations in cross flows with the duct tilted forward or at low speed maneuvering, with the duct nearly flat. A series of tests were conducted with the duct angle of attack varied between 5 deg and –25 deg. Maximum fan speed was 3000 rpm, corresponding to a tip speed of 497 ft/sec, and advance ratio ranged from 0 to 1.14.

Exit vane deflection angles from –40 deg to 40 deg were examined for both axial and forward flight test conditions.

Results and Discussion

Baseline performance characteristics were measured for axial and forward flight test conditions. Results from model geometry variations including the effects of flap deflection angle, flap chord length and duct chord length were obtained. Unless otherwise stated, performance results represent the combined duct and fan forces.
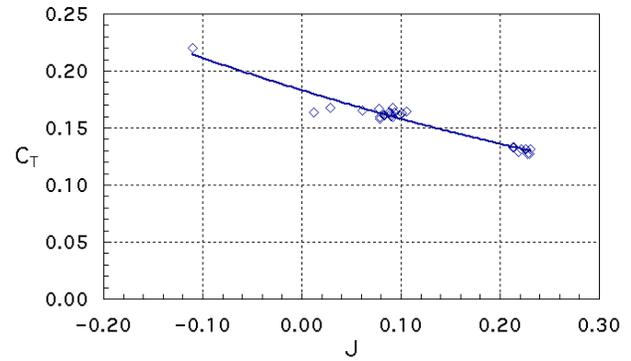
Axial

The thrust coefficient, power coefficient, and figure of merit are shown as functions of advance ratio in Fig. 4. The axial flow data, representing near static conditions, are clustered in two advance ratio regions, 0.05 to 0.10 and 0.20 to 0.25. The lower advance ratio range was a result of the fan outwash flow directed opposite of the wind tunnel normal flow direction as shown in Fig. 2a, producing a thrust coefficient of 0.16. The higher advance ratio range was the result of directing the fan outwash flow along the normal tunnel direction, α = -90 deg, which produced a 0.13 thrust coefficient. Figure 4b indicates minimal power coefficient scatter, and Fig. 4c shows an average near-hover figure of merit of about 50 percent.

Forward Flight

Baseline forward flight performance data are shown in Fig. 5. Propulsive force coefficient versus advance ratio for the full range of duct angle of attack as seen in Fig. 5a shows a positive propulsive force at low advance ratios for each duct angle of attack. As advance ratio increases, propulsive force decreases. As the ducted fan was adjusted to a more negative angle of attack, the propulsive force increased due to additional force from the forward component of the lift vector. Therefore, the combined forces were able to overcome the drag of the ducted fan. To maintain constant positive propulsive force with increasing advance ratio, the angle of attack must become more negative.
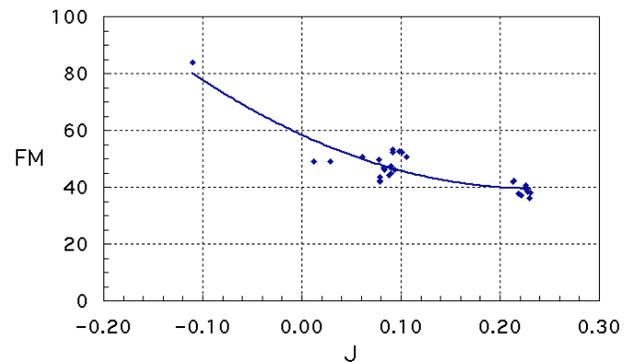
Power coefficient increases with increasing advance ratio (Fig. 5b). Reducing the duct angle of attack lowers the power coefficient. The flow appears to be separated over the duct lip at a duct angle of attack of 5 deg. Also, at 5-

a) **Thrust coefficient, shaft axis**
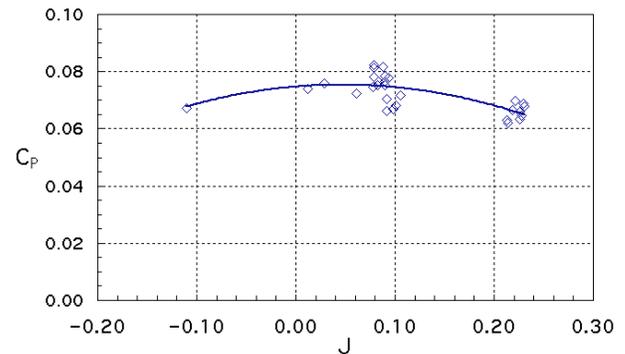
b) **Power coefficient**

c) **Figure of merit**

Fig. 4. Ducted fan thrust coefficient, power coefficient, and figure of merit as a function of advance ratio, axial flow, baseline configuration.

deg angle of attack, the power curve departs from the general trend of other tested angle of attack conditions.

Figure 5c shows that the lift coefficient. Initially the lift increases with increasing advance ratio. As the duct angle of attack becomes more negative, the thrust vector from the fan and duct is tilted more forward. Consequently, the vertical thrust component is lower, accounting for the reduction in lift as duct angle of attack decreases. At 5-

4

deg duct angle of attack, the lift coefficient is approximately equal to the 0-deg angle of attack data. This is the result of loss from the thrust vector, but gain from movement of the stagnation point on the duct. At –5-deg angle of attack, both the thrust vector and the stagnation point movement result in losses in the vertical component of thrust.
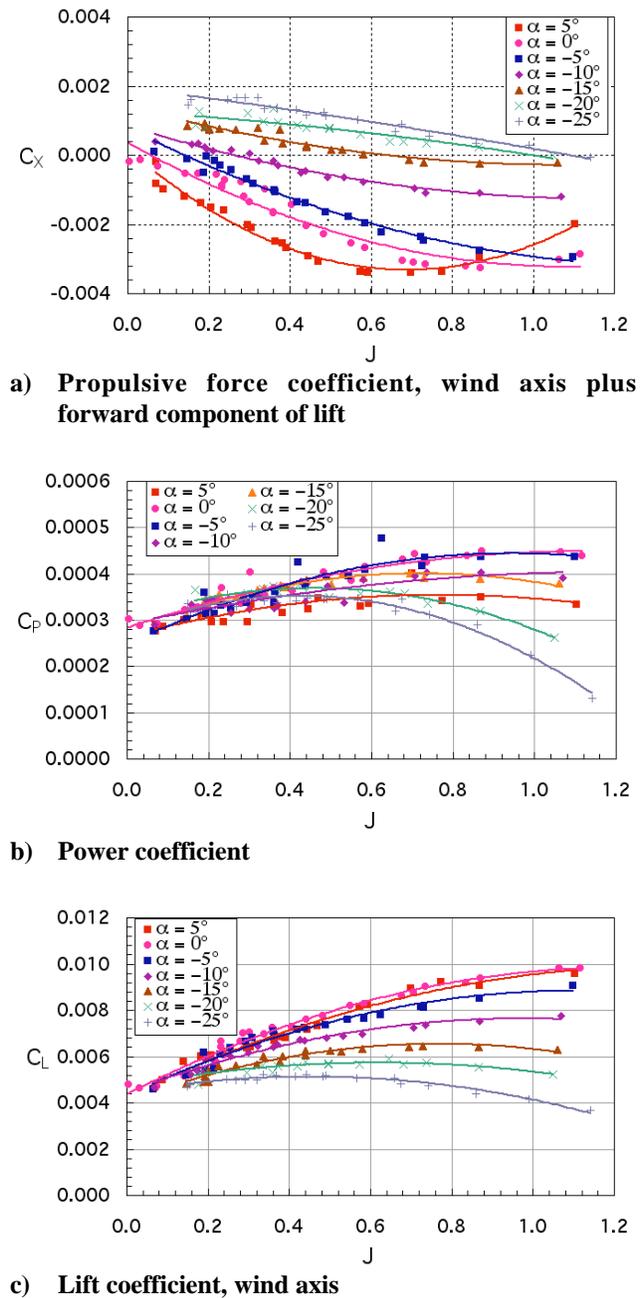

a) **Propulsive force coefficient, wind axis plus forward component of lift**

b) **Power coefficient**

c) **Lift coefficient, wind axis**

Fig. 5. Forward flight ducted fan performance versus advance ratio, baseline configuration.

Exit Vane Effectiveness
The exit vanes had two offsetting characteristics. Although the vanes add blockage to the downstream flow of the fan, they also assist in realigning the swirl component of the flow. A flapped vane, located at the duct exit can produce side forces. If the ducted fan is sufficiently above or below a vehicle's center of gravity, that side force can be used to produce control moments.

The side force coefficient for the 3-in exit vane with the 1.00-in and 2.25-in flaps was measured in axial flow test conditions (Fig. 6). The side force coefficient appears to increase as flap deflection angle increases. A slightly greater side force was produced by the 2.25-in flap, Fig. 6b, than the 1-in flap. Pitch, yaw and roll moment coefficients varied from –0.02 and +0.02.
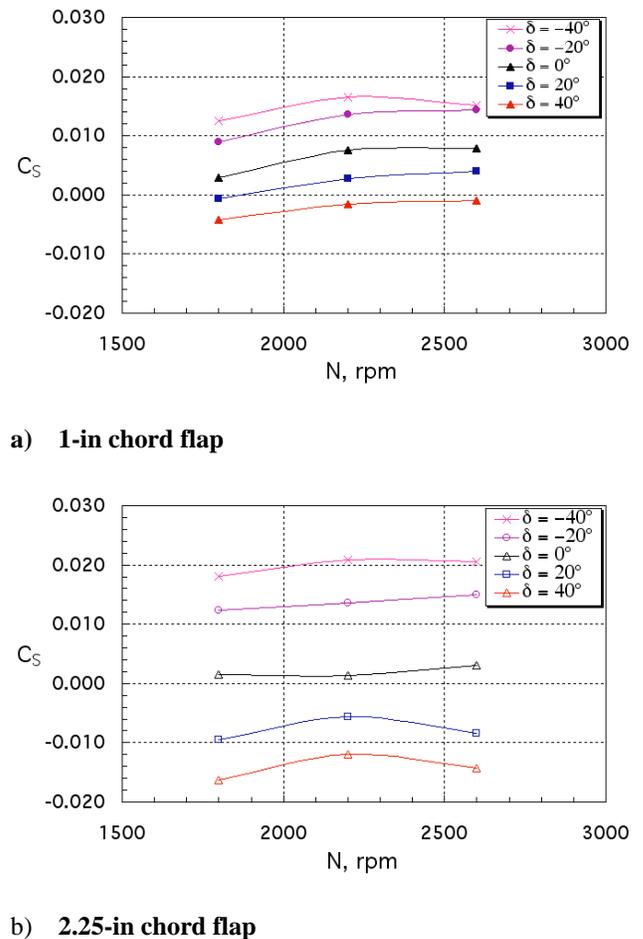

a) **1-in chord flap**

b) **2.25-in chord flap**

Fig. 6. Side force coefficient versus fan rotation speed, baseline configuration.

Duct Extension
Limited testing was performed to investigate the effect of increasing the duct chord length. A longer, 15-in chord, duct was created by adding a 5-in trailing edge sheet metal

5

extension to the baseline, 10-in chord, duct. Figure 7 shows the thrust coefficient for each duct versus advance ratio. Comparisons were made for axial flow conditions only. Extending the duct chord did not significantly effect the thrust coefficient.
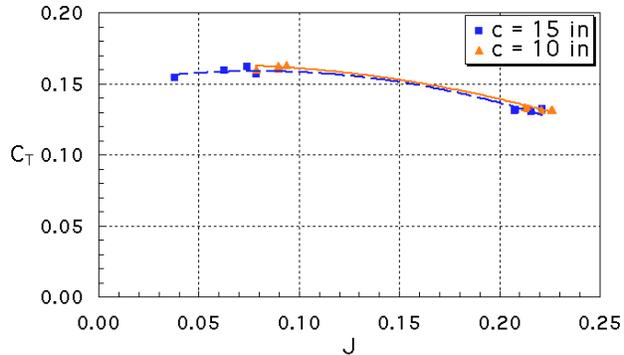
Fig. 7. Duct extension effect on thrust coefficient, axial flow conditions.

Conclusions

An experimental investigation was completed in the 7- by 10-Foot Wind Tunnel at NASA Ames Research Center to determine the performance characteristics of a ducted fan model. Axial and forward flight performance results were reported. The effects of variations in model geometry, such as exit vane flap deflection angle, flap chord length, and duct chord length were investigated. Specific finding and recommendations as a result of this investigation are as follows:

1) Axial flow data, representing near static conditions, produced an average thrust coefficient of 0.16 and an average figure of merit of about 50 percent.

2) Forward flight propulsive force results showed that in order to maintain constant positive propulsive force with increasing advance ratio, the duct angle of attack must become more negative. Also, as advance ratio increases, power coefficient increases. Decreasing the duct angle of attack lowers the power coefficient. At 5-deg angle of attack, the flow appears to be separated over the duct lip.

3) Exit vane flap deflection angle and flap chord length were shown to be effective methods of producing duct side force.

4) Extending the duct chord length did not significantly change the duct thrust coefficient.

6) Additional testing should be performed to research the effects of the non-uniform tip clearance.

7) Additional hover testing should be performed in a facility better representing hover conditions.

References

1) Moshier, M. and Bulaga, R., "Wind Tunnel Performance Investigation of the SoloTrek[TM] XFV[TM] Ducted Fan System," DARPA/DSO, Arlington,VA, 2001.
2) Stipa, L, "The Turbine Wing.", Reprinted from L'Aerotecnica, Vol. XI, No. 4, April, 1931. Translated under ONR Contract Nonr 978(01)
3) Sacks, A.H. and Burnell, J.A., "Ducted Propellers – A Critical Review of the State of the Art," Report No. ARD-232, Advanced Research Division of Hiller Aircraft Corporation, 1959.
4) Mort, K.W. and Yaggy, P.F., "Aerodynamic Characteristics of a 4-Foot-Diameter Ducted Fan Mounted on the Tip of a Semispan Wing," NASA TN D-1301, 1962.
5) Yaggy, P.F. and Mort, K.W., "A Wind-Tunnel Investigation of a 4-Foot-Diameter Ducted Fan Mounted on the Tip of a Semispan Wing," NASA TN D-776, 1961.
6) Yaggy, P.F. and Goodson, K.W., "Aerodynamics of a Tilting Ducted Fan Configuration," NASA TN D-785, March 1961.
7) Mort, K.W., "Performance Characteristics of a 4-Foot-Diamter Ducted Fan at Zero Angle of Attack for Several Fan Blade Angles," NASA TN D-3122, December 1965.
8) Mort, K.W. and Gamse, B., "A Wind Tunnel Investigation of a 7-Foot-Diameter Ducted Propeller," NASA TN D-4142, August 1967.
9) Black, D.M. and Wainauski, H.S., "Shrouded Propellers – A Comprehensive Performance Study," AIAA 5th Annual Meeting and Technical Display, Philadelphia, PA, October 1968.